Journal of Alloys and Compounds 619 (2015) 513–519

Contents lists available at ScienceDirect

Journal of Alloys and Compounds

journal homepage: www.elsevier.com/locate/jalcom

Effects of deep cryogenic treatment on the microstructure and mechanical properties of commercial pure zirconium

Chao Yuan, Yunpeng Wang, Deli Sang, Yijun Li, Lei Jing, Ruidong Fu *, Xiangyi Zhang

State Key Laboratory of Metastable Materials Science and Technology, Yanshan University, Qinhuangdao, Hebei 066004, PR China
College of Materials Science and Engineering, Yanshan University, Qinhuangdao, Hebei 066004, PR China

ARTICLE INFO

Article history:
Received 25 April 2014
Received in revised form 3 August 2014
Accepted 26 August 2014
Available online 16 September 2014

Keywords:
Metals and alloys
Deep cryogenic treatment
Microstructure
Mechanical properties
Zirconium

ABSTRACT

The effects of deep cryogenic treatment (DCT) on the microstructure and mechanical properties of commercial pure zirconium were investigated. Experimental results indicated that DCT induced a change in grain orientation and improved internal stress, which in turn increased dislocation density that led to improved hardness. Hardness in basal planes was found to be significantly larger than that in prism planes. Moreover, strength was enhanced in DCT-treated zirconium and the ductility was comparable to that of as-annealed zirconium. This phenomenon was due to the increase in dislocation density and the good ductility resulting from the motion of pre-existing dislocations and specific dislocation configurations. DCT led to the transformation of tensile fracture mode from mixed-rupture characteristics of quasi-cleavage and dimples to quasi-cleavage, thereby increasing compatible deformation capabilities. The possible mechanisms underlying microstructural modification, tensile strength, and hardness improvement were discussed.

1. Introduction

Cryogenic treatment is a very old process that is widely used for high-precision components. Shallow cryogenic treatment is set at low temperatures (about −80 °C), whereas deep cryogenic treatment (DCT) is set at near-liquid-nitrogen temperatures (about −196 °C). DCT improves certain properties beyond the enhancement obtained by normal cold treatment [1–3]. DCT is different from those methods of severe plastic deformation (SPD) processing at cryogenic conditions, such as cryogenic rolling, pinning and milling. Instead of nanostructured and ultrafine-grains in SPD-processed metals, the variation of crystal defect and phase transformation may play more important role in increasing of the properties of DCT-treated metals. Over the past few decades, the effects of various cryogenic treatments on the performance of steel have received considerable interest. DCT reportedly increases the normal temperature strength and hardness of steels [4,5], provides dimensional stability or microstructural stability [6], and improves wear [7–9] and fatigue resistance [10,11]. The improvement in mechanical properties can be ascribed to the complete transformation of retained austenite into martensite, precipitation of fine dispersed carbides, and removal of residual stresses [6,7,12]. Previous studies have shown that the hardness and abrasion resistance of DCT-treated samples evidently improve because of transformation of abundant retained austenite to martensite, secondary carbide precipitation [13], and the precipitation of nanosized η-carbides in primary martensite [14]. In addition, DCT combined with tempering treatment enables the enhancement of fatigue properties for the precipitation of fine carbides and the reduction in compressive residual stress [15].

Compared with studies on ferrous metals, research on the effect of DCT on nonferrous metals such as Mg, Al, and Ti alloys are limited. Asl et al. [2] found that after DCT, tiny laminar β phase particles almost dissolve, and the coarse divorced eutectic β phase extends into the neighboring matrix. As a result, the mechanical properties of AZ91 Mg alloy significantly improve. Jiang et al. [16] found that DCT induces the refinement of grains to approximately 0.1–3.0 μm, thereby improving the strength and elongation of 3102 Al alloy foil.

As aforementioned, evident changes in microstructure such as phase transformation or grain refinement have been verified for DCT-treated alloys. However, changes in microstructure and mechanical properties that can be introduced by DCT if no phase transformation occurs are worth investigating. In this study, coarse-grained zirconium (Zr) with a hexagonal close packed (hcp) structure and higher microstructure stability at cryogenic

* Corresponding author at: State Key Laboratory of Metastable Materials Science and Technology, Yanshan University, Qinhuangdao, Hebei 066004, PR China. Tel.: +86 335 858 7046; fax: +86 335 807 4545.
E-mail address: rdfu@ysu.edu.cn (R. Fu).

http://dx.doi.org/10.1016/j.jallcom.2014.08.201
0925-8388/

temperature was chosen as a model metal because of the limited deformation capability that results in easily saturated dislocation density [17]. Some unusual changes in mechanical properties were found in DCT-treated Zr, and the possible mechanisms in terms of microstructural modification were discussed.

2. Experimental

The material used in this study was commercial pure Zr plate (chemical composition summarized in Table 1). The plate was annealed in a vacuum at 1123 K for 4 h to obtain a homogeneous polycrystalline structure. The average grain size of the as-annealed sample was approximately 30–50 μm. The samples cut from the as-annealed plate were placed in a liquid nitrogen environment at 77 K for 24 h. Afterwards, the samples were taken out and cooled to room temperature.

X-ray diffraction (XRD) patterns of the as-annealed and DCT-treated samples were measured using a Rigaku D/max 2500 X-ray diffractometer (18 kW) with Cu Kα radiation (wavelength $\lambda = 1.54$ Å) in continuous-scanning mode over $2\theta = 30$–80° at a step of 0.02°. Differential scanning calorimetry (DSC) was conducted on a Diamond DSC (PerkinElmer Inc., UK). For dynamic scans, samples were subjected to temperatures ranging from 20 °C to −160 °C at a cooling rate of 20 °C/min. Microstructure features before and after DCT were observed by optical microscopy (OM), electron backscatter diffraction (EBSD), and transmission electron microscopy (TEM). EBSD analysis was performed using a HITACHI S-4800 scanning electron microscopy (SEM) system, whereas TEM observations were carried out with a JEOL-2010 TEM system at a voltage of 200 kV.

A FM-ARS9000 Vickers microhardness tester was used to measure the hardness of samples. Indentations were carried out with a given load of 200 g and a dwell time of 10 s. Hardness distributions over a square area of 4.5×4.5 mm^2, with a space between adjacent indentations of 0.5 mm were obtained. The tensile samples were machined with a gauge length of 30 mm and a cross-section of 10×1.5 mm^2. Four repeated tensile tests were performed on a MTS test system at a strain rate of 1×10^{-4} s^{-1} at room temperature under extensometer-measured strain control. Fracture surfaces after the tensile test were observed by SEM, and microstructures near the fracture surfaces were observed by TEM.

3. Results and discussion

3.1. XRD and DSC analyses

Fig. 1(a) shows the XRD patterns of as-annealed and DCT-treated samples. No phase transformation was observed in DCT-treated Zr compared with as-annealed Zr. However, the intensities of the diffraction peaks of DCT-treated Zr were slightly enhanced, which can be attributed to the variation in lattice constants caused by DCT. Changes in lattice constants were also observed in DCT-treated Mg [18,19]. To further confirm the microstructure stability of Zr at cryogenic temperature, a cryogenic DSC curve was obtained and is shown in Fig. 1(b). The smooth feature of the DSC curve indicated that no transformation occurred during DCT.

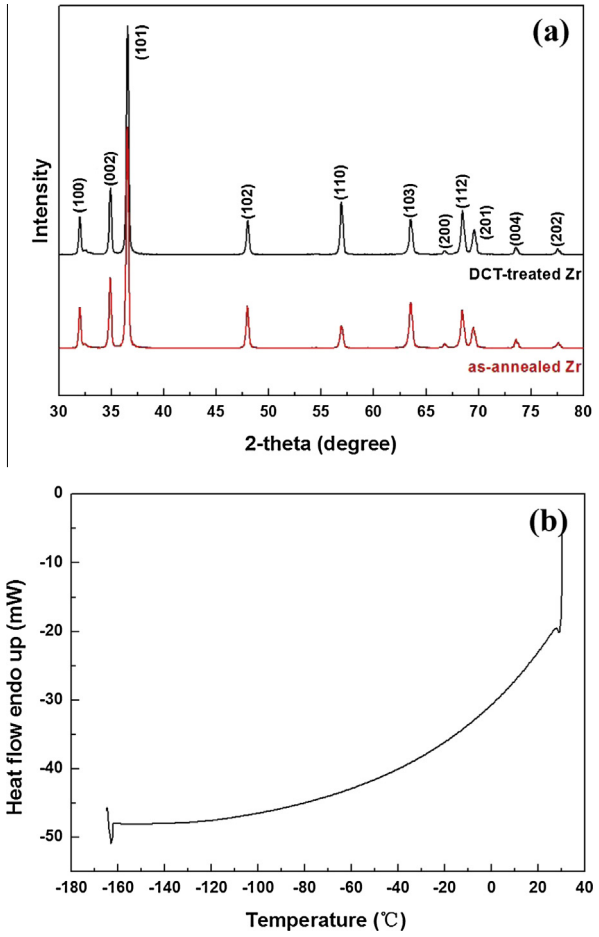

Fig. 1. XRD patterns of as-annealed and DCT-treated samples (a), and the cryogenic DSC curve of Zr (b).

3.2. EBSD analysis

To gain deep insight into microstructural changes, EBSD analysis was performed. In this analysis, orientation imaging microscopy (OIM) maps, inverse pole figure (IPF) maps, and boundary misorientation angle distributions were obtained before and after DCT, as shown in Fig. 2. Fig. 2(a) and (b) shows the OIM maps of Zr before and after DCT, with high-angle (HAGBs; grain boundary misorientations ⩾ 15°) and low-angle (LAGBs; grain boundary misorientations < 15°) grain boundaries depicted by black and white lines, respectively. The crystallographic directions corresponding to various colors can be inferred from the IPF triangle shown at the bottom right corner of Fig. 2(a) and (b). The microstructure was characterized by equiaxed grains and a higher fraction of HAGBs. No phase transformation and precipitation occurred during DCT, consistent with the XRD and DSC results. Fig. 2(c) and (d) shows the IPF maps of Zr before and after DCT, respectively. The maximum intensity indicated the number of random orientations. A strong preference was observed toward the (0001) orientation, which was corroborated by the OIM maps in Fig. 2(a) and (b). Furthermore, the intensity of prism planes was lower and the grain orientations were much closer to the (0001) basal plane orientation after DCT. This finding can be attributed to the ordered arrangement of atoms resulting from the small changes in lattice constants [18,19]. The misorientation angle distributions in Fig. 2(e) and (f) shows that the crystallite boundaries were mainly high angle in nature. The HAGB fractions of Zr before and after DCT were about 81.2% and 85.3% of the total grain boundary length, respectively. Thus, DCT improved the formation of HAGBs. The increase in HAGB fractions may be related to the extrinsic dislocations formed during DCT (Fig. 3). The extrinsic dislocations were probably easier to react with the dislocations in LAGBs [20,21]. Therefore, the accumulation and rearrangement of dislocations resulted in the transformation of LAGBs to HAGBs, leading to increased HAGB and decreased LAGB fractions.

Table 1
Chemical composition (in wt%) of the investigated pure Zr.

Fe + Cr	C	N	H	O	Hf	Zr
0.2	0.05	0.01	0.005	0.16	4.5	Balance

3.3. TEM observations

The TEM images of the samples before and after DCT are presented in Fig. 3. The dislocation density of the DCT-treated sample was apparently higher than that of the as-annealed sample. When the temperature dropped from room temperature to cryogenic